Accepted Manuscript

Biomass-derived porous carbon highly efficient for removal of Pb(II) and Cd(II)

Anqi Wang, Zhikeng Zheng, Ruiqi Li, Di Hu, Yiran Lu, Huixia Luo, Kai Yan

Please cite this article as: A. Wang, Z. Zheng, R. Li, D. Hu, Y. Lu, H. Luo, K. Yan, Biomass-derived porous carbon highly efficient for removal of Pb(II) and Cd(II), *Green Energy & Environment*, https://doi.org/10.1016/j.gee.2019.05.002.

Title: Biomass-derived porous carbon highly efficient for removal of Pb(II) and Cd(II)

Author names and affiliations:

1. Anqi Wang: Guangdong Provincial Key Laboratory of Environmental Pollution and Remediation Technology, School of Environmental Science and Engineering, Sun Yat-sen University, 135 Xingang Xi Road, Guangzhou, 510275, China, E-mail: wanganq5@mail2.sysu.edu.cn

2. Zhikeng Zheng: uangdong Provincial Key Laboratory of Environmental Pollution and Remediation Technology, School of Environmental Science and Engineering, Sun Yat-sen University, 135 Xingang Xi Road, Guangzhou, 510275, China, E-mail: zhengzhk5@mail2.sysu.edu.cn
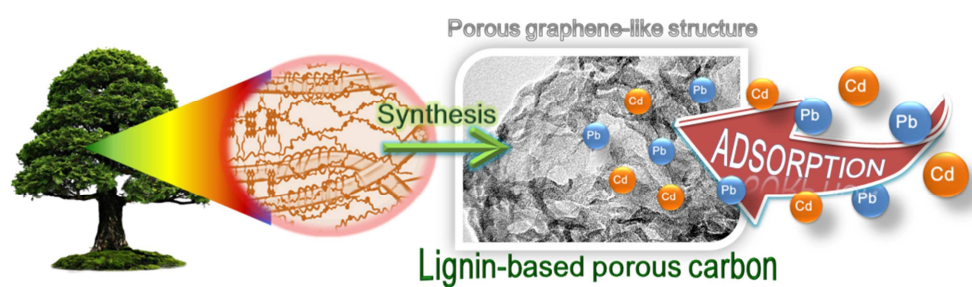
3. Ruiqi Li: Guangdong Provincial Key Laboratory of Environmental Pollution and Remediation Technology, School of Environmental Science and Engineering, Sun Yat-sen University, 135 Xingang Xi Road, Guangzhou, 510275, China, E-mail: lirq5@mail2.sysu.edu.cn

4. Di Hu: Guangdong Provincial Key Laboratory of Environmental Pollution and Remediation Technology, School of Environmental Science and Engineering, Sun Yat-sen University, 135 Xingang Xi Road, Guangzhou, 510275, China, E-mail: hudi5@mail.sysu.edu.cn

5. Yiran Lu: School of Engineering, Brown University, Providence, Rhode Island 02906, United States, E-mail: yiran_lu@brown.edu

6. Huixia Luo: School of Material Science and Engineering, Sun Yat-Sen University, 135 Xingang Xi Road, Guangzhou, 510275, China, E-mail: luohx7@mail.sysu.edu.cn

7. Kai Yan*: Guangdong Provincial Key Laboratory of Environmental Pollution and Remediation Technology, School of Environmental Science and Engineering, Sun Yat-sen University, 135 Xingang Xi Road, Guangzhou, 510275, China, E-mail: yank9@mail.sysu.edu.cn

Biomass-derived porous carbon highly efficient for removal of Pb(II) and Cd(II)

Anqi Wang[a], Zhikeng Zheng[a], Ruiqi Li[a], Di Hu[a], Yiran Lu[b], Huixia Luo,[c] Kai Yan[a,*]

[a] *Guangdong Provincial Key Laboratory of Environmental Pollution Control and Remediation Technology, School of Environmental Science and Engineering, Sun Yat-sen University, 135 Xingang Xi Road, Guangzhou 510275, China*

[b] *School of Engineering, Brown University, Providence, Rhode Island 02906, United States*

[c] *School of Material Science and Engineering, Sun Yat-Sen University, 135 Xingang Xi Road, Guangzhou, 510275, China*

*Corresponding author Email: yank9@mail.sysu.edu.cn

Abstract: The utilization of abundant and renewable biomass to fabricate advanced functional materials is considered a promising route for environmental applications. Herein, Lignin-based porous carbon with layered graphene-like structure (LPC) is successfully synthesized and applied to efficiently remove Pb(II) and Cd(II). The as-synthesized LPC materials are systematically characterized and these results show that LPC has a porous graphene-like structure, facilitating the diffusion and immobilization of heavy metal ions. The influence of different reaction parameters (solution pH, initial concentration of metal ions, contact time and adsorbent amount) on the adsorption performance is investigated in details. The results demonstrate that LPC can achieve superior adsorption capacities of 250.5 mg g^{-1} for Pb(II) and 126.4 mg g^{-1} for Cd(II), which are far superior to the previously reported adsorbents. Pseudo-second order kinetics model and Freundlich isotherm model describe the adsorption process well. Furthermore, the exhausted LPC can be regenerated easily

1

and exhibits the removal efficiency of 96% and 92% for Pb(II) and Cd(II) after five continuous runs, respectively. This study shows a sustainable strategy for the design of porous carbon material from naïve biomass and highlights the great potential in wastewater treatment.

1. Introduction

Nowadays, the massive discharge of heavy metal ions into the natural environment has become a major environmental issue because of their carcinogenicity, non-biodegradability and bioaccumulation [1-3]. Among the discharged heavy metal ions, Pb(II) and Cd(II) have been recognized as the typical hazardous contaminants, which can be enriched in human body along the food chain, resulting in irreparable harm to various organs, tissue, nervous and reproductive system even in trace amounts [4, 5]. Therefore, it is essential to develop an environmental-friendly and low-cost strategy to effectively remove these heavy metal ions from sewage and soil.

Numerous remediation techniques have been explored and applied in the treatment of heavy metals pollution, including ion-exchange, phase extraction, chemical precipitation, membrane separation, biological treatments and electrochemical methods [6-9]. However, the above-stated methodologies commonly suffer from a number of inherent limitations, such as low efficiency, long period, high cost, complex operation and generation of secondary pollution, which make them

difficult to obtain satisfactory results in practical application [10, 11]. Comparatively, adsorption method has received extensive attention and began to play a crucial role for the remediation of heavy metal pollution, due to its cost-effectiveness, high efficiency, simple operation as well as considerable choice for adsorbents [12, 13].

Recent studies have shown that the application of biomass-derived materials in the field of environmental pollution control has been frequently studied and made great progress [2, 11, 14-16]. Biomass-derived materials exhibit very attractive properties, e.g., renewable resources, carbon-neutral, low-cost, wide abundance, eco-friendly, mechanical stability, etc. [17, 18]. Especially, a number of biomass-derived materials have been chosen as the most promising adsorbents and employed to remove organic and inorganic pollutants, owing to the advantages of easy functionalization, large surface area and porous structure [19, 20]. As a most abundant biopolymer with high carbon content in nature, lignin can be largely available from the waste of agriculture, forestry and industry, thus it has been seen as a potential precursor to develop value-added carbon materials nowadays [21, 22]. However, to the best of our knowledge, most of the biomass-derived adsorbents were commonly prepared from carbohydrates (i.e., glucose) through the hydrothermal carbonization or activation method, and few studies focused on the removal of heavy metal ions with the naïve lignin-based materials.

Inspired by these studies, we attempt to develop a win-win strategy for simultaneously achieving the exploitation of biomass waste and the remediation of heavy metal pollution. The work shows a facile, green and efficient method for the

3

selective removal of Pb(II) and Cd(II) with several attractive features: (1) Layered graphene-like carbon (LPC) with porous structure was facilely prepared from lignocellulosic biomass; (2) The physicochemical properties of LPC were studied by SEM, EDS, TEM, XRD, XPS, BET, FTIR, Raman and Zeta potential analysis; (3) The as-obtained LPC was efficient for the selective removal of Pb(II) and Cd(II), where different parameters (i.e., solution pH, initial concentration of metal ions, contact time and adsorbent amount) were evaluated systematically; (4) The recyclability, adsorption isotherms, kinetics and mechanism were also investigated.

2. Experimental section

2.1. Material synthesis

The resources and purity of chemicals used in the experiment are provided in Supplementary Information (SI). The biomass-derived LPC adsorbent was prepared through the chemical solution combustion method using lignin as abundant and low-cost raw material. In a typical procedure, 1 g of lignin and 2 g of urea were dissolved into 20 mL of 3.8% ammonia solution under the continuous magnetic stirring until the homogenous distribution was obtained. Afterward, the mixture was then transferred into a beaker and dried at 80 °C for 1 h in an oven with Ar protecting environment. Subsequently, the as-obtained solid was milled into powders and calcined at 350 ^{o}C for 1 h with a heating rate of 5 ^{o}C min^{-1}, then heated at a rate of 5 ^{o}C min^{-1} to 500 ^{o}C for 1 h under Ar atmosphere. Finally, the biomass-derived LPC material with layered graphene-like structure was obtained after cooling down to

4

room temperature. For comparison, the carbon prepared from lignin using the same method without the addition of urea (abbreviated as L-A) and without the addition of urea and ammonia (named as L-C) were also synthesized.

2.2. Characterizations

The surface morphology of the as-prepared LPC was explored by scanning electron microscopy coupled with energy dispersive X-ray spectrometer (SEM/EDS, Hitachi S3200N), and the texture was investigated by transmission electron microscopy (TEM, JEOL JEM-3010) at 220 kV. X-ray diffraction spectrum (XRD) was obtained using a Rigaku D-MAX 2200 VPC powder diffractometer with Cu $K\alpha$ radiation at 40 kV and 26 mA, collecting the dataset over the range of 10-90° with a step width of 0.02^{o}/2θ. Raman measurement was carried out on Renishaw inVia Raman spectrometer. Fourier transform infrared spectroscopy (FTIR) was recorded on a PerkinElmer Spectrum One FTIR spectrometer in the range from 400 to 4000 cm^{-1}. The porosity information was measured using a Micromeritics ASAP 2020 adsorption apparatus, and prior to measurements, the prepared sample was activated in a vacuum at 200 ^{o}C for 12 h. The surface chemical valent was analyzed by X-ray photoelectron spectroscopy (XPS) using a Thermo ESCALAB 250 instrument with Al $K\alpha$ source. The surface zeta potential data of the adsorbent at different pH values were acquired by a NanoBrook Omni Zeta potential analyzer.

2.3. Adsorption experiment

The adsorption behavior of the obtained biomass-derived LPC materials was evaluated. The stock solution of Pb(II) and Cd(II) (1000 mg L^{-1}) were prepared by

dissolving 1.34 g PbCl$_2$ and 2.74 g Cd(NO$_3$)$_2$·4H$_2$O in 100 mL deionized water, respectively. All adsorption experiments were conducted in a conical flask (50 mL) waggled in a thermostated THZ-100 shaker (Shanghai YiHeng Scientific Instruments Co., Ltd., China) with a speed of 150 rpm under 30 $^{\circ}$C. To evaluate the adsorption performance in the solution with different pH values, 20 mg LPC adsorbent were added into 60 mg L^{-1} Pb(II) and 100 mg L^{-1} Cd(II) solution and the desired solution pH was adjusted by 0.1 M NaOH and HNO$_3$ solution with a pH meter (ST-3100, OHAUS). Different amounts of LPC (range from 5 to 40 mg) were used to treat 60 mg L^{-1} Pb(II) and Cd(II) solution (50 mL) with the pH value of 6 for Pb(II) and 2 for Cd(II). Therewith, 100 mg L^{-1} Pb(II) and Cd(II) solution were treated by 20 mg LPC adsorbent at different contact time varying from 0.1 to 10 h for the adsorption kinetic study. In the adsorption isotherm study, 20 mg LPC adsorbent was used to remove different concentrations of Pb(II) (from 10 to 200 mg L^{-1}) and Cd(II) (from 10 to 150 mg L^{-1}) at pH of 6, respectively.

After adsorption, the LPC material was separated by centrifugation, and the supernatant was analyzed using ICP-OES spectrometer to measure the concentrations of metal ions. The adsorption capacity q_t (mg g^{-1}) and removal percentage Y (%) of heavy metal ion can be calculated by Eqs. (1) and (2):

$$q_t = (C_0 - C_t)/W \times V \tag{1}$$

$$Y = 100(C_0 - C_t)/C_0 \tag{2}$$

where C_0 is the concentration of Pb(II) and Cd(II) in the initial solution (mg L^{-1}); C_t represents the Pb(II) and Cd(II) concentration in solution (mg L^{-1}) at adsorption time t;

V stands for the volume of Pb(II) and Cd(II) solution (L), and *W* denotes the mass of LPC adsorbent (g).

3. Results and discussion

3.1. Synthesis of LPC materials

The synthesis procedure of LPC was presented in Fig. 1. In this work, a new type of lignin-derived porous carbon adsorbent with layered graphene-like structure was prepared using lignin as the raw material. First, lignin was mixed with urea (Fig. 1a), where urea provided nitrogen source for doping into carbon-based materials [23, 24]. Besides, at high temperature, urea was decomposed into NH_3 to assist the formation of the porous structure [25]. Then the mixture was dissolved into ammonia which acted as activating agent and pore-expanding agent (Fig. 1b and c). Finally, the LPC material was dried, calcined at 350 ^{o}C for 1 h and then heated to 500 ^{o}C for 1 h under Ar (Fig. 1d). The internal structure, pore size distribution and specific surface area of LPC had been improved significantly compared with lignin precursor, which was promising for the removal of heavy metals.

SEM images of the as-synthesized lignin-derived porous carbon material were presented in Fig. 2a. It was clearly observed that the LPC adsorbent possessed a honeycomb-like structure comprised of thin layers with varying shape and size. The porous structure was clearly presented on the crude surface of LPC. The EDX analysis of LPC (Fig. S1) showed that it mainly contained C as the framework of LPC, and certain amounts of N were also detected. However, as shown in Fig. S2, the

7

carbon prepared from lignin without urea (L-C) was mainly composed of large chunk, showing particle-aggregated and dense irregular surface with few pores. The large bulk layered structure was observed on the surface of L-A sample (Fig. S2). The framework of the as-prepared LPC adsorbent was further examined by TEM. As shown in Fig. 2b-d, the single-/multi-layered porous structure is prominent throughout the sample. Besides, the lignin-derived porous carbon material exhibited a highly interconnected porous structure. Compared with previously reported sugar-derived carbon materials [16, 20, 26-29], the framework of LPC with specially layered graphene-like structure was quite attractive, which is mainly due to the role of urea and ammonia used in the modified chemical solution combustion method.

XRD patterns of the as-prepared LPC material were presented in Fig. 3a. A broad diffraction peak observed at ca. 22° was the typical peak of amorphous carbon. Similarly, the XRD analysis of L-C and L-A materials (Fig. S3) also mainly displayed a wide carbon diffraction peak at ca. 22°. Raman spectrum (Fig. 3b) showed two characteristic peaks appearing at 1344 and 1584 cm^{-1} attributed to D- and G-band, respectively. The D-band was related to the disorder and defects graphite structure, while the G-band was assigned to the sp^{2}-hybridized carbon forms [30, 31]. Besides, it is well known that the symmetric peak (2D) as an important parameter was used for the estimation of graphene layer numbers based on its shape and position. The broad and weak 2D band located at 2862 cm^{-1} suggesting the existence of the layered graphene-like structure in the LPC material. Typically, the spectral profile (i.e., peak position and intensity) can provide unique information to analyze the degree of

8

accumulation and graphitization of carbon material [32]. Compared with the L-C and L-A samples (Fig. S4), LPC possessed the sharp and ordered peaks, meaning that LPC had a higher graphitization degree with smaller thickness, which was well consistent with the SEM and TEM observation.

The BET surface area and pore size distribution of the layered graphene-like LPC were further analyzed by N_2 adsorption-desorption test. As shown in Fig. 3c, a classic type-IV adsorption isotherm with a hysteresis loop of type H2 was observed, indicating the existence of mesopores in the obtained LPC adsorbent. The main distributions of pore sizes were around 2.3 nm The BET specific surface area was determined to be 375.8 m^2 g^{-1} for LPC material. The FTIR analysis of the lignin and LPC samples were employed to study the change of chemical functional groups. As shown in Fig. 3d, the peak at 831 cm^{-1} for pristine lignin were assigned to the C-H out of plane vibration. The peak at 1116 cm^{-1} were arising from the p-hydroxyphenyl (H) units. The peaks at 1610 and 1509 cm^{-1} were related to the vibration of aromatic skeleton. The peaks at 2935 and 2839 cm^{-1} were attributed to the presence of C-H stretching [33]. Meanwhile, it can be observed that the obtained LPC contained new peaks at 1043, 1196, 1732 and 1536 cm^{-1} predominantly due to the stretching vibration of C-N and N-O [34], respectively, which confirmed the successful preparation of nitrogen doped LPC via the modified chemical solution combustion method. Moreover, a broad band centered around 3439 cm^{-1} appeared in the FTIR analysis of the lignin and LPC materials, corresponding to the O-H stretching vibration.

The surface element composition and electronic state of layered graphene-like LPC materials were further characterized by XPS (Fig. 4). The whole XPS survey spectra were shown in Fig. 4a, whereas the peaks of C, N, and O were clearly present. The C 1s spectra (Fig. 4b) can be split into two peaks, which corresponded to C-C (285-286 eV) and C-O (288.5-290 eV), respectively. The binding energy of N1s (Fig. 4c) appeared at 403.7 eV was ascribed to C-N-C. Furthermore, three peaks located at 529.6-529.9eV, 531.9-532.4eV and 533.00-533.31 eV were detected in the peak fitting of O 1s spectrum (Fig. 4d), which could be ascribed to lattice oxygen, surface adsorbed oxygen and textural water, respectively.

3.2. Influence of operating parameters on the adsorption

3.2.1. Influence of solution pH

The adsorption experiment of Pb(II) and Cd(II) was firstly performed using the synthesized LPC at different pH value. It was observed from Fig. 5a that the Pb(II) adsorption capacity of the porous biomass carbon LPC increased considerably with the increasing pH value. There was little change in the adsorption quantity when the pH becomes larger than 4. The sharply increasing adsorption capacity at the solution pH ranging between 3 and 4 was probably because of the competition of the Pb^{2+} with H_3O^+ for adsorption sites of LPC. On the other hand, the surface functional groups of LPC would be protonated and acquired positive charges, resulting in the electrostatic repulsion with cationic Pb^{2+}. As reported previously [35], the adsorption played the leading role in the removal of Pb(II) at the low pH, while pH was higher than 6, the precipitation process of $Pb(OH)_2$ could be gradually dominated the process. At neutral

10

or higher pH condition, the adsorption of LPC would occur concurrently with precipitation of heavy metal ions, the pH value was thus set to 6 in this study.

As shown in Fig. 5b, with the gradual increase of solution pH, the adsorption capacity of LPC for Cd(II) constantly increased, and the maximum adsorption appeared at a pH of 9. Among different Cd(II) species, Cd^{2+} was the dominant species when pH value was less than 8 in the solution. When the pH value was over 8, more cadmium ion would be converted to precipitate instead of adsorption removal by the fabricated porous carbon material. Therefore the pH value was set at 6 for the adsorption process of Cd(II).

3.2.2. Effect of adsorbent amount

As shown in Fig. 5c, a sharp rise in the Pb(II) removal efficiency can be seen clearly with the mass ratio of absorbent/heavy metal ions increased in the initial stage, following with a slow increase at the amount of 30 mg. Similarly, the adsorption quantity of Cd(II) increased with the increase of LPC amount variation from 10 to 50 mg (Fig. 5d). This was because effective adsorption sites on the LPC surface significantly increased as the adsorbent amount raised, leading to the rapid removal of Pb(II) and Cd(II) from aqueous solution. However, when the adsorbent amount continued to increase, the removal efficiency of heavy metal ions will reach equilibrium.

3.2.3. Effect of contact time and adsorption kinetics

The experimental results to determine the effect of contact time on the adsorption of Pb(II) and Cd(II) were presented in Fig. 6a. It was evident that there was a rapid

increase in the Pb(II) and Cd(II) removal efficiency from 0 to 250 mg g^{-1} and from 0 to 127 mg·g^{-1}, respectively, with the increase of contact time ranging from 0 to 60 min. When the contact time was more than 60 min, a plateau appeared, and further prolonging the contact time had only a trivial effect on the removal of Pb(II) and Cd(II). This could be ascribed to the saturation of adsorption sites on the surface of LPC adsorbent.

The adsorption kinetics was analyzed for a better understanding of the adsorption mechanism by LPC. The experimental data were fitted using the pseudo-first-order and pseudo-second-order model, respectively (Fig. 6b and c), and the calculated kinetic parameters and correlation coefficients (R^2) were given in Table S1. The linear forms of pseudo-first-order and pseudo-second-order model were depicted in Eqs. (3) and (4). It was shown that the pseudo-second-order equation was well fitted with the obtained results compared with the pseudo-first-order equation, where the best correlation coefficient ($R^2 \geq 0.99$) was obtained, suggesting that the rate controlling step in this study may be the chemical adsorption.

$$\log(Q_e - Q_t) = \log Q_e - \frac{k_1 t}{\ln 10} \tag{3}$$

$$\frac{t}{Q_t} = \frac{t}{k_2 Q_e^2} - \frac{1}{Q_e} t \tag{4}$$

where Q$_e$ and Q$_t$ are the amounts of adsorbed metal ions (mg g^{-1}) at equilibrium and at any time, k_1 and k_2 are pseudo-first order model (min^{-1}) and pseudo-second-order model (g mg^{-1} min^{-1}) rate constants, respectively.

3.2.4. Effect of initial concentration and adsorption isotherms

The relationship between the initial concentration of heavy metal ions and the

adsorption performance of the resulting adsorbent were further investigated. The adsorption of Pb(II) and Cd(II) by LPC versus the initial concentration curves are presented in Fig. 7. The rapid adsorption process has taken place at the lower concentration, which could be owing to the adequate adsorption sites on the LPC surface. With the increasing of initial concentration, adsorption sites were gradually occupied by metal ions and then reached the status of saturation ultimately.

The adsorption values of LPC toward Pb(II) and Cd(II) were investigated with Langmuir (Eq. (5)) and Freundlich (Eq. (6)) isotherms. Fig. 7 showed that the Freundlich isotherm fitting curves were well matched with actual values of Pb(II) and Cd(II) adsorption under the studied operating conditions. Besides, the relevant parameters listed in Table S2 illustrated that the maximum R^2 values (0.988 for Pb(II) and 0.975 for Cd(II)) can be obtained in Freundlich model, which confirmed that the adsorption process of Pb(II) and Cd(II) can be well described using the Freundlich model with the heterogeneous adsorption behavior.

$$\frac{C_e}{q_e} = \frac{1}{q_m K_L} + \frac{C_e}{q_m} \tag{5}$$

$$\ln q_e = \frac{1}{n} \ln C_e + \ln K_F \tag{6}$$

where K_L (L mg^{-1}) and q$_m$ (mg g^{-1}) are the Langmuir isotherm parameters relating the adsorption energy and the equilibrium adsorption capacity, respectively. K_F (mg (L mg^{-1})$^{-1/n}$) and n are the Freundlich isotherm parameters representing the adsorption capacity and the adsorption intensity, respectively.

3.3 Desorption and recyclability of LPC

The desorption behaviors and recyclability of LPC were further studied. In this

13

work, four desorbents (i.e., HNO_3, EDTA, $NaNO_3$ and Na_2CO_3) with the concentration of 0.1 mol L^{-1} were selected, and the results were shown in Table S3. Albeit the optimal desorbent was HNO_3, a high concentration of HNO_3 would destroy the structure of LPC. Therefore, 0.1 mol L^{-1} Na_2CO_3 solution was used as the desorbent.

The recycling performance of LPC for adsorption of Pb(II) and Cd(II) was evaluated, as shown in Fig. 8. After the adsorption, the LPC material was separated through centrifugation and then dried for the next round. Thus, the regeneration procedure unavoidably caused the weight loss of the LPC. However, the removal efficiencies of Pb(II) and Cd(II) were still higher than 96% and 92% after successive five cycles of the adsorption-regeneration process, respectively. The excellent recyclability as well as a simple regeneration method made the LPC as a potential adsorbent to remove Pb(II) and Cd(II) from wastewater.

3.4 Comparison of adsorption property of different materials

Fig. S5 showed the removal efficiency of Pb(II) and Cd(II) in a solution (50 mL) with the concentration of 60 mg L^{-1} after 200 min treatment using 20 mg of LPC, L-A, L-C and pure lignin at pH of 6. Compared to the results of L-A, L-C and lignin, the obtained LPC displayed an superior removal efficiency of Cd(II) (98.3%) and Pb(II) (99.2%), which was ~8.2 and 6.3 times higher than that of pristine lignin (Cd(II) (12.1%) and Pb(II) (15.6%)), respectively.

To benchmark the adsorption capacity of LPC, the previously reported adsorbents are summarized and compared in Table 1. Generally, compared with other

14

adsorbents, the synthesized LPC with larger surface area exhibited superior performances for Pb(II) and Cd(II) removal with less adsorbent amount, higher initial concentrations, shorter contact time, and under the near-natural condition. More importantly, the LPC can be synthesized through a simple chemical solution combustion method by using the renewable lignin, which not only avoided the contamination from the harmful precursors but also reduced the energy consumption as well as the operating cost in water remediation.

3.5 Mechanism study

The adsorption mechanism of the as-fabricated LPC material for heavy metal ions removal was further explored through analysis of the Zeta potential and XPS data. Firstly, the adsorption LPC performance increased with the increase of pH, which was attributed to the electrostatic interaction between the LPC surface and heavy metal ions as confirmed by the zeta potential analysis (Fig. S6). Specifically, the LPC exhibited positive potentials when pH was lower than 3, while its surface potential was negative as pH increased from 3 to 9 resulting in the enhanced adsorption efficiencies for Pb^{2+} and Cd^{2+} via the electrostatic attraction. XPS analysis of the LPC material after adsorption was further performed (Fig. S7). The appearance of strong peaks centered at 406.1 and 412.1 eV correspond to Cd 3d, and the distinctive peaks observed near 138.1 and 144.1 eV were assigned to Pb 4f. These data demonstrated that Pb(II) and Cd(II) ions were complexed or precipitated on the surface of LPC adsorbent, suggesting that the high surface area and porous graphene-like structure of LPC were beneficial for the removal of heavy metal ions. In general, the high surface

15

area and electrostatic interaction played a crucial role in the adsorption process of heavy metal ions on the LPC.

4. Conclusions

In this work, a novel kind of cost-effective and environmental-friendly porous carbon with layered graphene-like structure was prepared using the sustainable lignin as the raw material. The physicochemical properties of LPC were investigated using multiple characterization techniques (i.e., Zeta potential, XRD, Raman, FT-IR, BET, EDX, XPS, SEM and TEM), confirming the fabricated LPC had a porous structure with graphene-like thin layers. The LPC material display very promising performance for the removal of Pb(II) and Cd(II) with the optimal adsorption capacities of 250.47 and 126.37 mg g^{-1}, respectively. An obvious dependence on the solution pH was found for the removal of Cd(II) over the pH ranged from 2 to 9, whereas a little influence was observed for the removal of Pb(II) when the pH was higher than 6. The kinetic analysis showed the adsorption process obeys a pseudo-second-order model, indicating that the chemical adsorption is the rate controlling step. The isotherm of adsorption process can be well fitted to Freundlich model, suggesting the heterogeneous adsorption behavior. Moreover, the LPC adsorbent demonstrated satisfactory recyclability and the removal efficiency of Pb(II) and Cd(II) were more than 96% and 92% even after five continuous runs. The porous carbon from the renewable biomass proves as a good candidate for clean recovery of heavy metals from wastewater. This study may promote the valorization of abundant biomass for the remediation of the environmental pollutants.

Acknowledgments

References

[1] J. Gong, T. Liu, X. Wang, X. Hu, L. Zhang, Environ. Sci. Technol. 45 (2011) 6181-6187.

[2] S. Hokkanen, A. Bhatnagar, M. Sillanpää, Water Res. 91 (2016) 156-173.

[3] R. Li, W. She, Y. Lu, D. Hu, K. Yan, Gen. Chem. 5 (2019) 180024.

[4] J. Liang, X. Li, Z. Yu, G. Zeng, Y. Luo, L. Jiang, Z. Yang, Y. Qian, H. Wu, ACS Sustain. Chem. Eng. 5 (2017) 5049-5058.

[5] L. Ma, Q. Wang, S.M. Islam, Y. Liu, S. Ma, M.G. Kanatzidis, J. Am. Chem. Soc. 138 (2016) 2858-2866.

[6] I. Heidmann, W. Calmano, J. Hazard.Mater. 152 (2008) 934-941.

[7] F. Fu, Q. Wang, J. Environ. Manage. 92 (2011) 407-418.

[8] L. Fang, L. Li, Z. Qu, H. Xu, J. Xu, N. Yan, J. Hazard.Mater. 342 (2018) 617-624.

[9] Y. Zou, X. Wang, A. Khan, P. Wang, Y. Liu, A. Alsaedi, T. Hayat, X. Wang, Environ. Sci. Technol. 50 (2016) 7290-7304.

[10] S. Deng, P. Wang, G. Zhang, Y. Dou, J. Hazard.Mater. 307 (2016) 64-72.

[11] G. Lin, S. Wang, L. Zhang, T. Hu, J. Peng, S. Cheng, L. Fu, J. Clean. Prod. 192 (2018) 639-646.

[12] B. Xiang, D. Ling, H. Lou, H. Gu, J. Hazard.Mater. 325 (2017) 178-188.

[13] X.Y. Yu, T. Luo, Y.X. Zhang, Y. Jia, B.J. Zhu, X.C. Fu, J.H. Liu, X.J. Huang, Acs Appl. Mater. Inter. 3 (2011) 2585-2593.

[14] L. Zhou, C. Richard, C. Ferronato, J.M. Chovelon, M. Sleiman, Chem. Eng. J. 334 (2018) 2098-2104.

[15] K. Yan, C. Jarvis, J. Gu, Y. Yan, Renew. Sustain. Energy Rev. 51 (2015) 986-997.

[16] F.J. García-Mateos, R. Ruiz-Rosas, M.D. Marqués, L.M. Cotoruelo, J. Rodríguez-Mirasol, T. Cordero, Chem. Eng. J. 279 (2015) 18-30.

[17] K. Yan, Y. Liu, Y. Lu, J. Chai, L. Sun, Catal. Sci. Technol. 7 (2017) 1622-1645.

[18] E.N. Yargicoglu, B.Y. Sadasivam, K.R. Reddy, K. Spokas, Waste Manage. 36 (2015) 256-268.

[19] A.R. Betts, N. Chen, J.G. Hamilton, D. Peak, Environ. Sci. Technol. 47 (2013) 14350-14357.

[20] W.J. Liu, Y.Y. Wang, L.L. Ling, H. He, Y.R. He, H.Q. Yu, H. Jiang, Environ. Sci. Nano 3 (2016).

[21] Y. Xi, Y. Wang, D. Yang, Z. zhang, W. Liu, Q. Li, X. Qiu, J. Alloy. Compd. 785 (2019) 706-714

[22] X. Kang, A. Kirui, M.C.D. Widanage, F. Mentink-Vigier, D.J. Cosgrove, T. Wang, Nat. Commun. 10 (2019) 347.

[23] K. Yan, G. Wu, C. Jarvis, J. Wen, A. Chen, Appl. Catal. B: Environ. 148-149 (2014) 281-287.

[24] A. Wang, Y. Lu, Z. Yi, A. Ejaz, K. Hu, L. Zhang, K. Yan, ChemistrySelect. 3 (2018) 1097–1101.

[25] A. Wang, H. Wang, H. Deng, S. Wang, W. Shi, Z. Yi, R. Qiu, K. Yan, Appl. Catal. B: Environ. 248 (2019) 298-308.

[26] H. Liu, F. Xu, Y. Xie, C. Wang, A. Zhang, L. Li, H. Xu, Sci. Total Environ. 645 (2018) 702-709.

[27] Q. Chen, J. Zheng, L. Zheng, Z. Dang, L. Zhang, Chem. Eng. J. 350 (2018) 1000-1009.

[28] A. Wang, H. Li, J. Xiao, Y. Lu, M. Zhang, K. Hu, K. Yan , ACS Sustain. Chem. Eng. 6 (2018), 15995-16000.

[29] B. Li, L. Yang, C.Q. Wang, Q.P. Zhang, Q.C. Liu, Y.D. Li, R. Xiao, Chemosphere 175 (2017) 332-340.

[30] W. Han, L. Chen, W. Song, S. Wang, X. Fan, Y. Li, F. Zhang, G. Zhang, W. Peng, Appl. Catal. B: Environ. 236 (2018) 212-221.

[31] R. Zhang, M. Ma, Q. Zhang, F. Dong, Y. Zhou, Appl. Catal. B: Environ. 235 (2018) 17-25.

[32] Y.B. Xi, D.J. Yang, X.Q. Qiu, H. Wang, J.H. Huang, Q. Li, Ind. Crop. Prod. 124 (2018) 747-754.

[33] P. Asawaworarit, P. Daorattanachai, W. Laosiripojana, C. Sakdaronnarong, A. Shotipruk, N. Laosiripojana, Chem. Eng. J. 356 (2019) 461-471.

[34] M. Graglia, J. Pampel, T. Hantke, T.P. Fellinger, D. Esposito, ACS Nano 10 (2016) 4364-4371.

[35] Z.H. Diao, J.J. Du, D. Jiang, L.J. Kong, W.Y. Huo, C.M. Liu, Q.H. Wu, X.R. Xu, Sci. Total Environ. 642 (2018) 505-515.

[36] M.K. Mondal, J. Environ. Manage. 90 (2009) 3266-3271.

[37] C. Zhang, J. Sui, J. Li, Y. Tang, W. Cai, Chem. Eng. J. 210 (2012) 45-52.

[38] S. Wang, B. Gao, Y. Li, A. Mosa, A.R. Zimmerman, L.Q. Ma, W.G. Harris, K.W. Migliaccio, Bioresource Technol. 181 (2015) 13-17.

[39] T. Zhao, Y. Yao, D. Li, F. Wu, C. Zhang, B. Gao, Sci. Total Environ. 640-641 (2018) 73-79.

[40] A. Shahat, H.M.A. Hassan, H.M.E. Azzazy, E.A. El-Sharkawy, H.M. Abdou, M.R. Awual, Chem. Eng. J. 332 (2018) 377-386.

[41] F. Zhang, X. Wang, D. Yin, B. Peng, C. Tan, Y. Liu, X. Tan, S. Wu, J. Environ. Manage. 153 (2015) 68-73.

18

[42] M. Ruthiraan, N.M. Mubarak, R.K. Thines, E.C. Abdullah, J.N. Sahu, N.S. Jayakumar, P. Ganesan, Korean J. Chem. Eng. 32 (2015) 446-457.

[43] A. Sari, M. Tuzen, Appl. Clay Sci. 88-89 (2014) 63-72.

[44] J. Wu, D. Huang, X. Liu, J. Meng, C. Tang, J. Xu, J. Hazard.Mater. 348 (2018) 10-19.

[45] M. Iqbal, A. Saeed, S.I. Zafar, J. Hazard.Mater. 164 (2009) 161-171.

[46] A.B. Nastasović, B.M. Ekmeščić, Z.P. Sandić, D.V. Ranđelović, M. Mozetič, A. Vesel, A.E. Onjia, Appl. Surf. Sci.385 (2016) 605-615.

[47] J. Deng, Y. Liu, S. Liu, G. Zeng, X. Tan, B. Huang, X. Tang, S. Wang, Q. Hua, Z. Yan, J. Colloid Inter. Sci. 506 (2017) 355-364.

Figure Captions
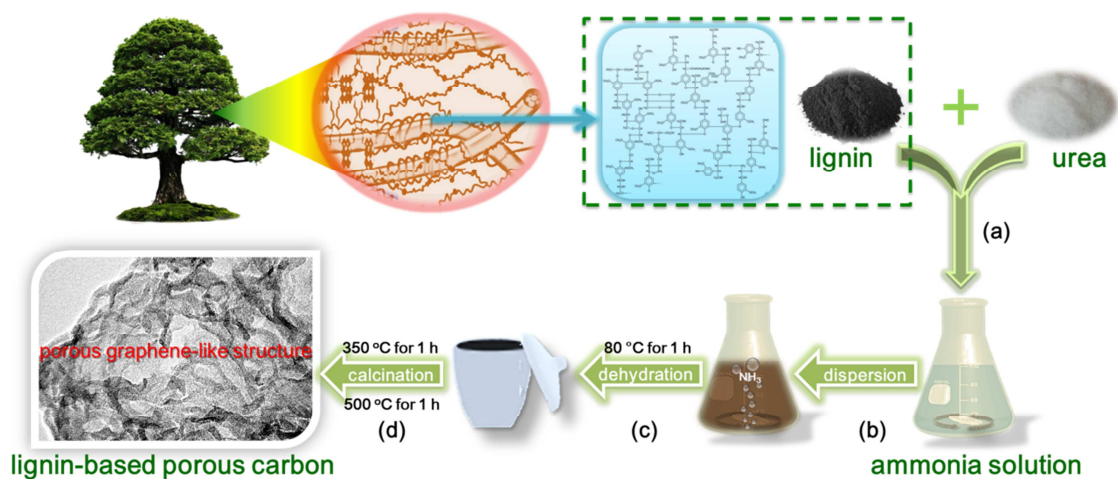
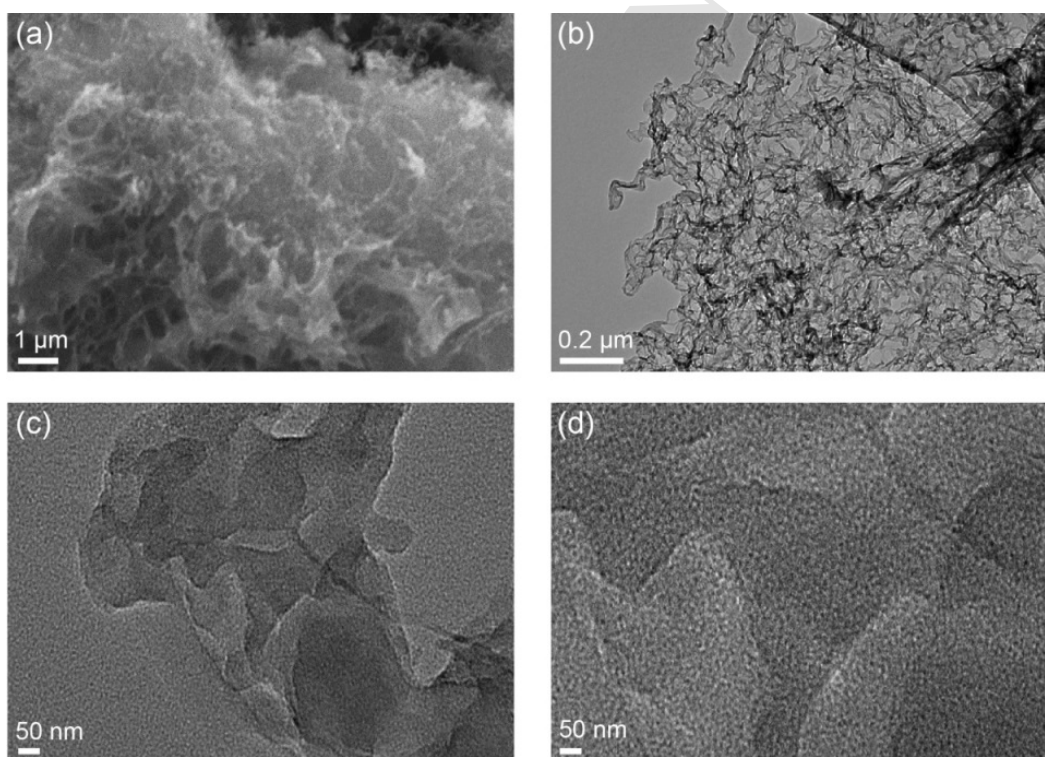**Fig. 1.** Schematic illustration for the synthesis of LPC.

Fig. 2. SEM (a) and TEM (b-d) images of the as-prepared LPC adsorbent.
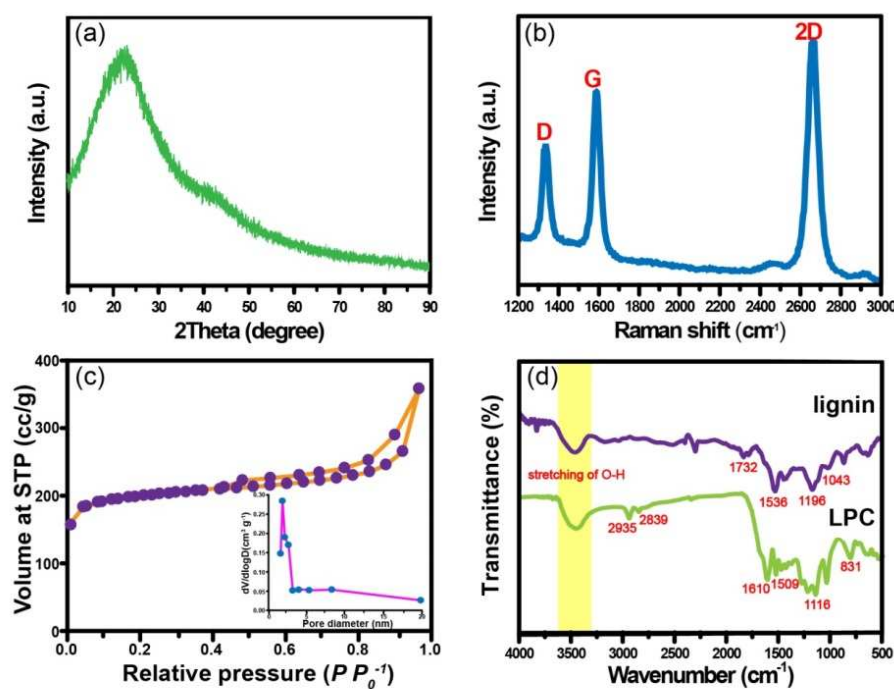
Fig. 3. XRD pattern (a); Raman spectrum (b); N$_2$ adsorption-desorption analysis of LPC (c) (Inset: corresponding pore size distributions); FTIR spectra (d) of lignin and LPC.
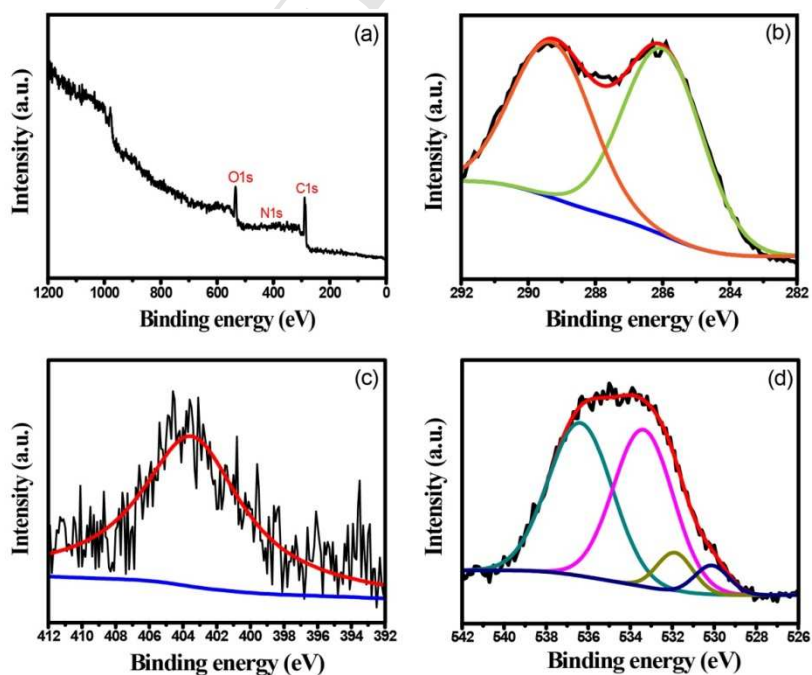

Fig. 4. XPS spectra of LPC adsorbent: (a) XPS survey; (b) C1s; (c) N1s; (d) O1s.
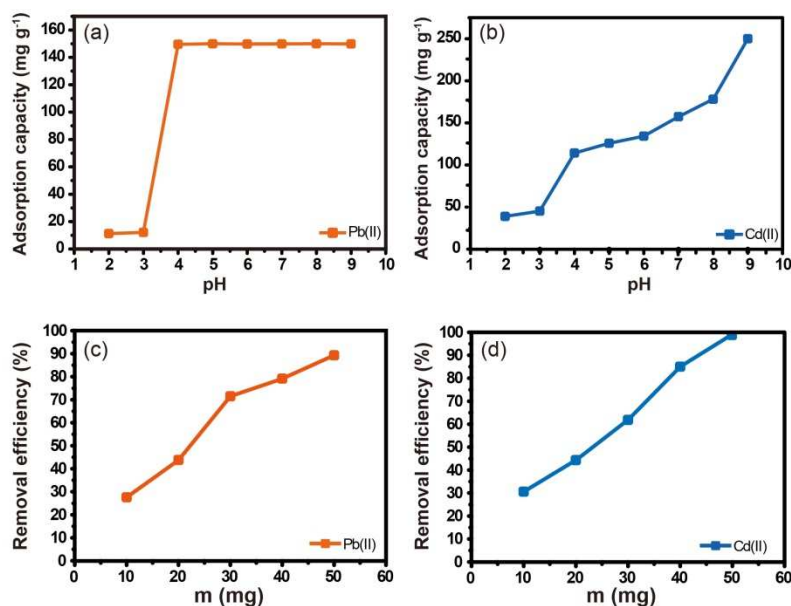
21

Fig. 5. Effect of pH value (a-b) and adsorbent amount (c-d) on the adsorption of Pb(II) and Cd(II) using LPC.
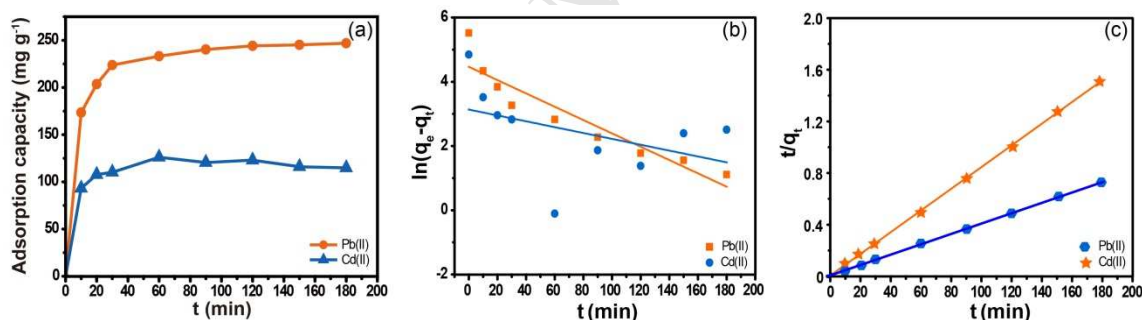

Fig. 6. Effect of contact time on the adsorption of Pb(II) and Cd(II) by LPC (a). Pseudo-first-order (b) and pseudo-second-order (c) kinetic for the adsorption of Pb(II) and Cd(II) on LPC.
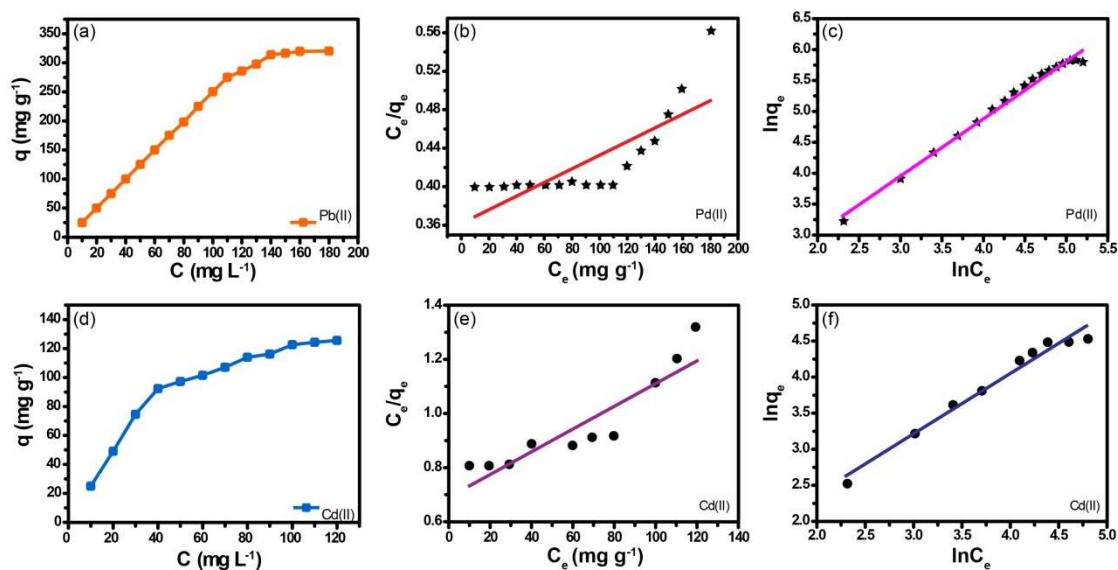
22

Fig. 7. Effect of initial concentration on the adsorption of Pb(II) and Cd(II) by LPC (a

and d). Adsorption isotherms Pb(II) and Cd(II) onto LPC: Langmuir model (b and e),

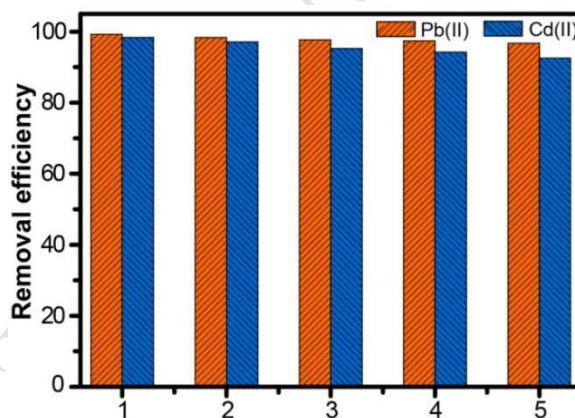Freundlich model (c and f).

Fig. 8. The cycle performance of LPC in the adsorption of Pb(II) and Cd(II).

[Experimental conditions: Initial concentration $C_0 = 60$ mg L^{-1}, pH = 2 (Cr (VI)) and

= 6 (Pb(II)), t = 200 min, LPC = 0.4 g L^{-1}].

23

Table 1

Comparison of Pb(II) and Cd(II) maximum adsorption capacity of LPC with those of various previously studied adsorbents.

Adsorbents	Heavy metals	Adsorption capacity	Refs.	Adsorbents	Heavy metals	Adsorption capacity	Refs.
Activated tea waste	Pb(II)	81.00 mg g^{-1}	[36]	MnO-Kaol	Cd(II)	36.47 mg g^{-1}	[43]
				Kaol	Cd(II)	14.11 mg g^{-1}	
CNT/thiol	Pb(II)	65.52 mg g^{-1}	[37]	BC-MnO$_x$	Cd(II)	81.10 mg g^{-1}	[29]
Biochar/manganosite	Pb(II)	4.91 mg g^{-1}	[38]	Ca-MBC	Cd(II)	10.07 mg g^{-1}	[44]
Bhar/birnessite	Pb(II)	47.05 mg g^{-1}					
Pomelo peel biochar	Pb(II)	88.74 mg g^{-1}	[39]	Mango peel waste	Pb(II)	99.05 mg g^{-1}	[45]
					Cd(II)	68.90 mg g^{-1}	
DMTD loaded MSNs	Pb(II)	67.20 mg g^{-1}	[40]	PGME-deta	Pb(II)	164.00 mg g^{-1}	[46]
					Cd(II)	152.00 mg g^{-1}	
Water hyacinth biochar	Cd(II)	70.30 mg g^{-1}	[41]	CPMB	Pb(II)	8.26 mg g^{-1}	[47]
					Cd(II)	24.68 mg g^{-1}	
Mnetic biochar	Cd(II)	62.50 mg g^{-1}	[42]	**LPC**	**Pb(II)**	**250.47 mg g^{-1}**	**This**
FMWCNTs	Cd(II)	83.33 mg g^{-1}			**Cd(II)**	**126.37 mg g^{-1}**	**work**

No conflict of interest exits in the submission of this manuscript, and this manuscript is approved by all authors for submission. I declare on behalf of my co-authors that the work described is original research that has not been published previously.